INSPECTION OF SPRAY ON FOAM INSULATION (SOFI) USING AND MICROWAVE AND MILLIMETER WAVE SYNTHETIC APERTURE FOCUSING AND HOLOGRAPHY

J.T. Case[1], F.L. Hepburn[2], R. Zoughi[1]

[1]Applied Microwave Nondestructive Testing Laboratory (*amntl*)
Electrical and Computer Engineering Department
University of Missouri-Rolla, Rolla, MO 65409, USA

[2]NASA George C. Marshall Space Flight Center
Huntsville, AL 35812, USA

Keywords: microwave, millimeterwave, nondestructive testing, foam, SOFI

INTRODUCTION

The Space Shuttle Columbia's catastrophic failure is thought to have been caused by a dislodged piece of external tank spray on foam insulation (SOFI) striking the left wing of the orbiter causing significant damage to some of the reinforced carbon/carbon leading edge wing panels [1]. Microwave and millimeter wave nondestructive evaluation methods have shown great potential for inspecting SOFI for the purpose of detecting anomalies such as small air voids that may cause separation of the SOFI from the external tank during a launch [2,3]. These methods are capable of producing relatively high-resolution images of the interior of SOFI. Although effective, there are some advantages in using synthetic focusing methods as opposed to real focusing methods such as reduced probe size, the ability to determine depth from multiple views, and the ability to slice images due to sufficient range resolution. To this end, synthetic aperture focusing techniques (SAFT) were first pursued for this purpose and later wide-band microwave holography was implemented [4-7].

This paper presents the results of this investigation using frequency domain synthetic aperture focusing technique (FD-SAFT) and wide-band microwave holography methods illustrating their potential capabilities for inspecting the space shuttle's SOFI at millimeter wave frequencies.

PROPOSED APPROACH

Samples were interrogated by measuring the vector microwave reflection coefficient at the aperture of an open-ended rectangular waveguide at K-band (18-26.5 GHz). Using an Agilent PNA Series Network Analyzer (E8361A), the measurements were either single frequency or the frequency was swept throughout the available bandwidth. As shown in Fig. 1, the rectangular waveguide probe followed a raster path such that all measurement points were made at $z = 0$ and the sample was placed below at some distance $z = -h$. Two image processing methods were used to process the raw microwave data, namely FD-SAFT and wide-band microwave holography [4,6].

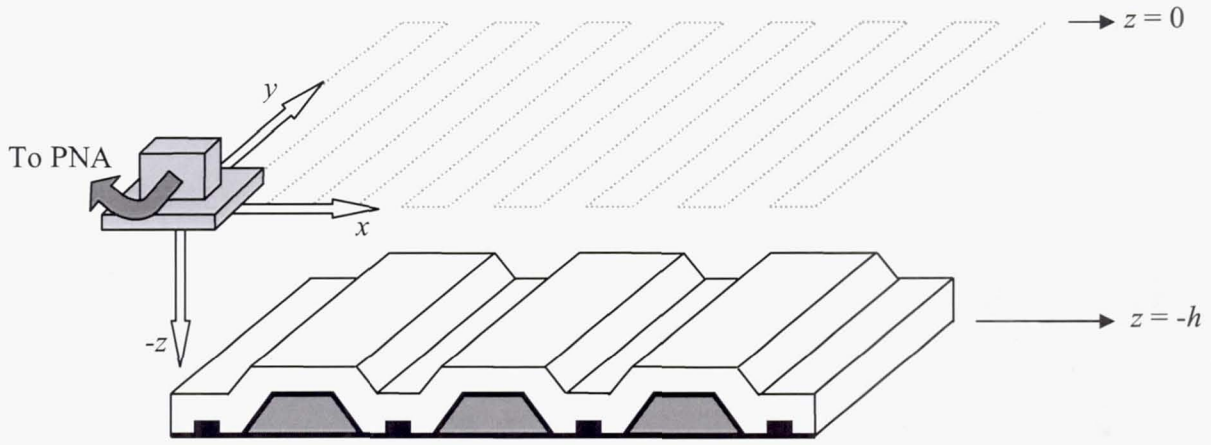

FIGURE 1. Illustration of scanning procedure with open-ended rectangular waveguide probe on an underlying SOFI sample.

A. Narrow-Band FD-SAFT

The first method pursued was FD-SAFT, which is synthetic aperture focusing technique applied in the frequency domain [4]. The first derivation pursued was L.J. Busse's narrow-band version in which the data is assumed to be single frequency and is based on angular spectrum decomposition [7]. The raw data is measured at $z = 0$ and is contained in:

$$f(x, y : z = 0)$$

such that

$$0 \le x \le x_{\max} \text{ and } 0 \le y \le y_{\max}$$

and such that f is sampled at discrete locations in x and y (see Fig. 1). Subsequently, this must be decomposed onto a plane wave spectrum using the 2-D Fast Fourier transform:

$$F(k_x, k_y : z = 0) = FFT_{2D}\{f(x, y : z = 0)\}$$

The ranges for k_x and k_y are centered about $k_x = 0$ and $k_y = 0$. Next, the data is propagated to the plane $z = -h$ such that the sample under test will be brought into focus. This is done by using the two-way backward wave propagator:

$$B(z, \omega) = \exp\left[i2kz\left(1 - \left(k_x / 2k \right)^2 - \left(k_y / 2k \right)^2 \right) \right]$$

such that ω is the radial frequency of operation and $k = \omega / c$. The intermediate quantity F' after applying the backward wave propagator is defined as:

$$F'(k_x, k_y : z = -h) = F(k_x, k_y : z = 0) \cdot B(z = -h, \omega)$$

The last step is to project the data back to real space using the inverse 2-D Fourier transform:

$$s(x, y : z = -h) = FFT_{2D}^{-1}\{F'(k_x, k_y : z = -h)\}$$

The processed data, $s(x, y : z = -h)$, is a single frequency high-resolution focused image at height $z = -h$. The spatial resolution of this image is roughly half the dimension of the antenna aperture similar to a focused synthetic aperture radar (SAR) [8].

Further extensions of this method included averaging over multiple frequencies either in the spatial or spatial frequency domains [4], neither of which improved the image especially if the object exceeded the depth of focus of the synthetically focused beam. Also, the multiple frequency auto-focusing technique (MF-AFT) was explored, but this focuses on the largest reflection available in the time domain [9]. This method was rejected since the goal was to find small reflections between air and SOFI rather than large reflections like SOFI to aluminum substrate. For this reason, a method was sought that would provide higher range resolution along the *z*-direction. This method was wide-band microwave holography.

B. Wide-Band Microwave Holography

The second method used is wide-band microwave holography [6]. It is similar in concept to FD-SAFT initially, and it also uses angular spectrum decomposition. The raw data measured at $z = 0$ is contained in:

$$f(x, y, \omega)$$

such that:

$$0 \le x \le x_{\max} \text{ and } 0 \le y \le y_{\max}$$

and such that f is sampled at discrete locations in x and y and at discrete frequencies, ω. The goal is to transform the raw data to the 3-D holographic representation $s(x, y, z)$.

The first step is to decompose the data onto a plane wave spectrum as before, and this must be done independently for every frequency using the 2-D Fourier transform:

$$F(k_x, k_y, \omega) = FFT_{2D}\{f(x, y, \omega)\}.$$

Again, the ranges for k_x and k_y are then centered about $k_x = 0$ and $k_y = 0$. Using the dispersion relation:

$$k_x^2 + k_y^2 + k_z^2 = (2k)^2 = \left(2\frac{\omega}{c}\right)^2$$

one can relate k_z to ω such that:

$$k_z = k_z(\omega) = \sqrt{\left(2\frac{\omega}{c}\right)^2 - k_x^2 - k_y^2}$$

where imaginary values are ignored. This results in the dataset $F(k_x, k_y, k_z)$.

However, the spacing of k_z is not uniform after this transformation and the dataset must be resampled to a uniform distribution of k_z using interpolation methods. A fast linear interpolation scheme was used for this paper. After the necessary resampling was performed the dataset is now

$F'(k_x, k_y, k_z)$.

To attain the processed 3-D holographic representation, $s(x, y, z)$, simply a 3-D inverse Fourier transform must be performed:

$$s(x, y, z) = FFT_{3D}^{-1}\{F'(k_x, k_y, k_z)\}.$$

PRELIMINARY RESULTS

The two methods discussed, FD-SAF and wide-band microwave holography, were used on a 70 mm thick SOFI slab with 25 mm (1 in) diameter flat bottom holes drilled at the following depths: 25 mm (1 in), 19 mm (3/4 in), 13 mm (1/2 in), 6 mm (1/4 in), and 3 (1/8 in). This slab was arranged in three different ways for two cases: 1) backed by substrate and 2) covered by 70 mm thick blank SOFI and backed by substrate. In this way the locations of the holes within the overall SOFI thickness varied. Liftoff, the distance between the probe and the SOFI surface, was 10 mm. Measurements were taken at K-Band (18-26.5 GHz) at sampling increments of 2 mm using an Agilent 8361A PNA Series Vector Network Analyzer.

For calculation purposes, three assumptions are made. First, the sample under test was assumed to not disperse or depolarize the incident wave. Secondly, it is assumed that only single reflections occur and no multiple reflections exist. Lastly, although we seek to detect the small reflection between the air and SOFI boundary, the wave traveling through the SOFI is assumed not to delay significantly because the dielectric properties of SOFI and air are so similar. This last assumption allows us to use the existing algorithms with no modification regarding traveling waves through media.

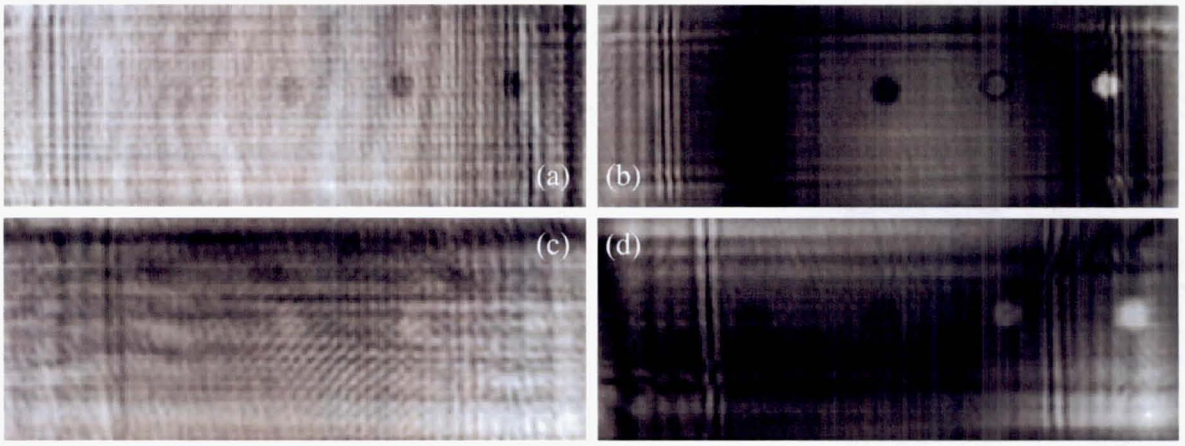

FIGURE 2. Flat bottom hole voids in foam: (a) case 1: SAFT processing at 22.25 GHz focusing at 74 mm from measurement plane; (b) case 1: microwave holography slice at 74 mm (18-26.5 GHz); (c) case 2: SAFT processing at 22.25 GHz focusing at 152 mm; (d) case 2: microwave holography slice at 152 mm.

In the first case where only one SOFI slab is used, FD-SAFT and wide-band microwave holography allow four of the five features to be seen, see. Fig. 2a and 2b. Only the last and least deep hole on the left is not seen. However, on closer inspection of the holography data for adjacent slices of data, the last hole, although dominated by edge effects, can be observed as a persistent signature. In the second case, unfortunately for FD-SAFT, the signature is blurred out

in the z-direction and is far too faint to observe because narrow-band FD-SAFT has no range resolution to accentuate a small signal. However, wide-band microwave holography does. For direct comparison between FD-SAFT and wide-band holography, the image processed with each method is displayed in Fig. 2c and 2d, respectively. Four of the five holes are again detected even under 140 mm (~ 5 ½ in) of SOFI.

The same methods will soon be applied at higher frequencies such as Ka-Band from 26.5 to 40 GHz or V-band from 50 to 75 GHz. These higher frequency bands will offer increased spatial and range resolutions. Also, samples more resembling the structure of the fuselage of the space-shuttle will be used including common features that aid the structural integrity of the fuselage.

ACKNOWLEDGEMENT: Funding for this work was provided by the NASA Marshall Space Flight Center through a Cooperative Agreement.

REFERENCES

[1] Columbia Accident Investigation Board Report, NASA, August 2003.

[2] S. Kharkovsky, F. Hepburn, J. Walker, R. Zoughi. "Nondestructive Testing of the Space Shuttle External Tank Foam Insulation using Near-Field and Focused Millimeter Wave Techniques," *Materials Evaluation* **63**, N5, 516-522 (2005).

[3] S. Shrestha, S. Kharkovsky, R. Zoughi and F. Hepburn. "Microwave and Millimeter Wave Nondestructive Testing of the Space Shuttle External Tank Insulating Foam," *Materials Evaluation* **63**, N3, 339-344 (2005).

[4] L.J. Busse, "Three-Dimensional Imaging Using a Frequency-Domain Synthetic Aperture Focusing Technique," *IEEE Transactions on Ultrasonics, Ferroelectrics, and Frequency Control* **39**, No. 2, 174-179 (1992).

[5] J.T. Case, J. Robbins, S. Kharkovsky, F. Hepburn, and R. Zoughi, "Microwave And Millimeter Wave Imaging of the Space Shuttle External Fuel Tank Spray On Foam Insulation (SOFI) Using Synthetic Aperture Focusing Techniques (SAFT)," *To appear in the Proceedings of the Thirty-second Annual Review of Progress in Quantitative Nondestructive Evaluation,* (2006).

[6] D.M. Sheen, D.L. McMakin, T.E. Hall, "Three-Dimensional Millimeter-Wave Imaging for Concealed Weapon Detection," *IEEE Transactions on Microwave Theory and Techniques* **49**, No. 9, (2001).

[7] J.W. Goodman, *Introduction to Fourier Optics*, New York: McGraw-Hill, 1968

[8] F.T. Ulaby, R.K. Moore and A.K. Fung, "Microwave Remote Sensing, Active and Passive" Vol. II, Artech House, Norwood, MA, 1986.

[9] Ahmed, Yamani, "Three-Dimensional Imaging Using a New Synthetic Aperture Focusing Technique," *IEEE Transactions on Ultrasonics, Ferroelectrics, and Frequency Control* **44**, No. 4, (1997).